

The Radio and IR Luminosity Function of compact Galactic HII regions

Roberta Paladini¹, Gianfranco DeZotti², Alberto Noriega-Crespo¹, Sean J. Carey¹,
MIPSGAL Team

ABSTRACT

We present the radio luminosity function (LF) of compact Galactic HII regions, derived by using ~ 200 sources from the recombination line survey by Caswell & Haynes (1987). The data set is complete for $S_{\text{peak}} > 1.3$ Jy at 5 GHz, corresponding to an integrated flux density of ~ 3 Jy. The LF is reconstructed by means of a generalized Schmidt's estimator which takes into account the actual spatial distribution of the HII regions along the plane of the Galaxy. The resulting LF is described by a two-component power-law, with a cut-off at $\log L(\alpha) = \sim 38.3$ erg/sec. This work will be complemented with the derivation, by means of the MIPSGAL data set, of the IR counterpart of the radio LF here presented.

An extension of this work will consist in deriving the IR counterpart of the radio LF here obtained, by making use of the MIPSGAL data set.

Subject headings: luminosity function, HII regions, radio continuum

1. Introduction

Massive stars play a fundamental role in the economy of a galaxy: by injecting in the Interstellar Medium (ISM) large quantities of energy and material, they provide a substantial contribution in shaping its global structure and evolution. In the early phases of their formation, massive stars of OB spectral type ($M > 8 M_{\odot}$, $L > 10^2 L_{\odot}$, lifetime $\sim 10^7$ yr)

¹Spitzer Science Center, California Institute of Technology, 1200 East California Boulevard, MC 220-6, Pasadena, CA 91125, USA

²INAF - Osservatorio Astronomico di Padova, Vicolo dell'Osservatorio 5, I-35122 Padova, Italy

produce the so-called HII regions, i.e. regions of ionized gas surrounding the central stellar associations. Here, we describe how we have derived the luminosity function (LF) for *compact* Galactic HII regions which, compared to the *ultracompact* HII population, are characterized by larger linear sizes (> 1 pc), a relatively low electron density n_e ($n_e \sim 10^2 \text{ cm}^{-3}$) and correspond to a later evolutionary stage in which the ionized region has expanded and partly freed from the parent dust cocoon.

Extensive studies of the LF of HII regions in external galaxies, mostly based on H_α observations, have established that: 1) the slope of the LF is correlated with Hubble type, with early-type galaxies having a steeper slope ($a \sim 2.0$)¹ than late-types ($a \sim 1.7$) (Kennicutt, Edgar & Hodge 1989, hereafter KEH89); 2) the LF becomes significantly flatter at low luminosities (KEH89; Rand 1992; Rosaz et al. 2000; Bradley et al. 2006). Variations of the LF in spiral arm versus inter-arm regions are controversial: some studies claim that the LF of interarm HII regions is steeper (KEH89; Banfi et al. 1993; Rand 1992), but others do not support this conclusion (Rozas et al. 1996; Knapen et al. 1997).

Investigations of the LF of HII regions in our own Galaxy suffer from two main limitations: 1) the samples are small and a large fraction of sources are affected by the solar distance ambiguity; 2) the strong inhomogeneity of the spatial distribution of the sources was not properly taken into account.

2. Sample selection

The aim of the present analysis is to derive the LF of compact Galactic HII regions improving on previous studies in two basic respects: 1) the use of a well-defined data set in terms of flux density completeness and kinematic information; 2) the use of a realistic model for the spatial distribution of HII regions.

Paladini et al. (2003; hereafter Paper I) collected a radio catalog of 1442 compact Galactic HII regions for which angular diameters and flux densities at a reference frequency, namely 2.7 GHz, are given. Despite the wealth of information contained in such a vast database, assessing its flux density completeness is very complicated, given that the catalog is constructed by combining data obtained with different instruments observing at different frequencies and angular resolution. Since this study requires a data set complete above a well-defined flux threshold, we decide not to make use of this catalog and rather look up the literature for available recombination lines data on compact Galactic HII regions.

¹ $N(L) \propto A L^{-a}$

The vast majority of catalogued HII regions is located in the first ($0^\circ < l < 90^\circ$) and fourth ($270^\circ < l < 360^\circ$) Galactic quadrants. The two major radio recombination lines surveys of compact HII regions in the first quadrant are those by DWBW and Lockman (1989). Other data sets have either lower completeness levels or smaller sky coverage. Both DWBW and Lockman claim to be complete for $S_{\text{peak}} > 1 \text{ Jy}^2$, although Lockman reports that ~ 200 sources are observed for the first time. This fact could be explained with misidentifications in the previous surveys. Nonetheless it appears rather puzzling.

The situation in the fourth quadrant is clearer. The region $210^\circ < l < 360^\circ$, $|b| < 2^\circ$ has been uniformly covered by the Caswell & Haynes (1987, hereafter CH87) survey. This survey, with an angular resolution of $\sim 4.1'$, represents the follow-up of the continuum 5 GHz survey by Haynes et al. (1978, 1979) and consists in H109 α and H110 α recombination lines measurements. All the sources with brightness temperature exceeding 1 K are included in the survey. This corresponds to a completeness limit, in peak flux density at 5 GHz, of 1.3 Jy. Given the sky coverage and well-defined characteristics of the survey, we choose the CH87 data set to perform our analysis.

CH87 observed 316 compact HII regions in total. Of these, we keep the sources satisfying two main criteria. First, we select the sources with a measured radial velocity $|V_{\text{LSR}}| \geq 10$ km/s. This allows the exclusion of objects whose radial velocities may be strongly affected by peculiar velocity components, and thus are not usable to estimate their distance from the rotation curve. In addition, we reject sources with 5 GHz peak flux below the completeness limit, i.e. with $S_p < 1.3 \text{ Jy}$.

The application of the above criteria leaves us with 166 compact HII regions. For each source, we compute the galactocentric and solar distances, R and D, respectively, by combining the hydrogen recombination line velocity measured by CH87 with the rotation curve by Fich, Blitz & Stark (1989). We have adopted $R_0 = 8 \text{ kpc}$, favoured by recent determinations (Eisenhauer et al. 2005).

As for the solar distances, part of the HII regions of the sample are affected by the well-known distance degeneracy problem. In this case, we proceed as in Paladini et al. 2004 (hereafter Paper II), using auxiliary (optical or absorption) data, when available, to break the degeneracy. For sources lacking such data we make use of the luminosity-physical diameter correlation found in Paper II and, in particular, of eq. (7) in that paper.

²Peak flux density at 4.8 GHz

3. The LF for an inhomogeneous source distribution

In this section we describe the approach adopted for our analysis. Under the assumption that the LF is independent of position, the number $N(L)$ of HII regions with luminosity L within $d \log L$ detected above a flux threshold S is related to the LF, $\phi(L) d \log L$, by:

$$N(L) d \log L = \phi(L) d \log L \int_0^{D_{\max}(S|L)} dD D \int_{l_{\min}}^{l_{\max}} dl n(R) \int_{z_{\min}}^{z_{\max}} dz \rho(z) \quad (1)$$

with $R = (R_0^2 + D^2 - 2DR_0 \cos l)^{1/2}$. In the above expression $n(R)$ and $\rho(z)$ describe the radial and vertical density profiles, respectively, and the multiple integral on the right-hand side is the *effective volume* within which a source of luminosity L is included in the catalog, i.e.:

$$V_{\text{eff}}(L|S) = \int_0^{D_{\max}(S|L)} dD D \int_{l_{\min}}^{l_{\max}} dl n(R) \int_{z_{\min}}^{z_{\max}} dz \rho(z) \quad (2)$$

where $D_{\max}(S|L) = (L/4\pi S)^{1/2}$, $z_{\max} = D \sin(b_{\max}) \simeq D b_{\max}$ and $z_{\min} = D \sin(b_{\min}) \simeq D b_{\min}$. If z_{\max} is much larger than the vertical scale length h or σ_z and $z_{\min} = -z_{\max}$, the integral over dz gives $\simeq 2h$ (for an exponential profile) or $\simeq (2\pi)^{1/2} \sigma_z$ (for a Gaussian profile). From eqs. (1) and (2) we can define a generalized Schmidt's estimator for the LF:

$$\phi(L) \Delta \log L = \sum_i \frac{1}{V_{\text{eff}}(L|S)} \quad (3)$$

where the sum is over all sources with luminosity within the interval $\Delta \log L$ around L . In eq. (2), for the vertical density profile we adopt a function of the form:

$$\rho(z|R) = \exp[-0.5(z/\sigma_z)^2] \quad (4)$$

Sanders et al. (1984) find [their eq. (5)] that the scale height of giant molecular clouds, assuming a Gaussian profile, scales as

$$z_{1/2} = 26R^{0.47} \text{ pc}, \quad (5)$$

where $z_{1/2} = (2 \ln 2)^{1/2} \sigma_z$. Since this relation is also consistent with the range of values (39 to 52 pc) quoted in Paper II for compact HII regions in our Galaxy we adopt it.

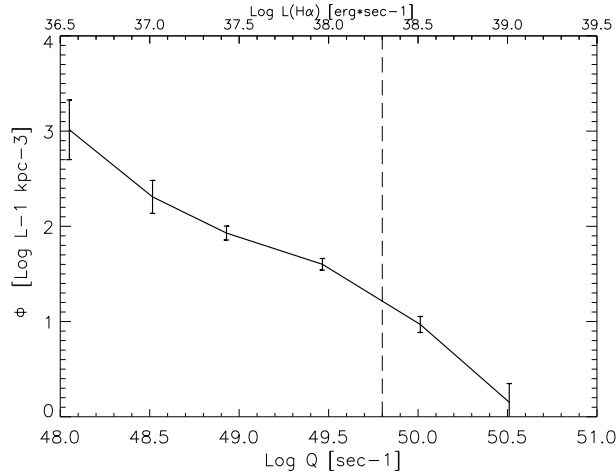


Fig. 1.— LF of compact HII regions from the CH87 sample expressed in units of Lyman continuum flux and H α luminosity. The error bars are computed as root-mean-square of the counts in each luminosity bin. Also plotted (dashed line) is the cut-off luminosity.

The radial density profile is more complex. The radial distribution of HII regions in the 4th quadrant is characterized by two peaks, with an artificial dip at $R \sim 8$ kpc due to having removed, from the original CH87 sample, the sources with measured velocity $|V_{\text{LSR}}| < 10$ km/sec which are located in correspondence of the solar circle. However, a bimodal distribution is expected because of the presence of the Scutum-Crux and Sagittarius spiral arms within the considered coordinate range. Based on this, we model $n(R)$ as the sum of two Gaussian distributions:

$$n(R) = R \left\{ \exp \left[-\left(\frac{R - R_{pk1}}{\sigma_{r1}} \right)^2 \right] + A \exp \left[-\left(\frac{R - R_{pk2}}{\sigma_{r2}} \right)^2 \right] \right\} \quad (6)$$

where R_{pk1} , R_{pk2} , σ_{r1} , σ_{r2} and A are free parameters to be determined fitting the observed distribution of sources as a function of the galactocentric distance R , given by:

$$\mathcal{N}(R) \Delta R = n(R) R \Delta R \int_{\theta_{\min}(R)}^{\theta_{\max}(R)} d\theta \quad (7)$$

$$\int_{z_{\min}(R,\theta)}^{z_{\max}(R,\theta)} dz \rho(z, R) \int_{\log L_{\min}(R,\theta)}^{\log L_{\max}} d \log L \phi(L)$$

To the number of parameters within a manageable limit, we adopted, in eq. (9), the usual power-law representation for the luminosity function $\phi(L) d \log L \propto L^{-1} d \log L$, after having checked that the results are little affected by changes of its slope within the currently

accepted range. The estimate of $\phi(L)$ is thus based on an iterative approach: we use a first guess on the shape of $\phi(L)$ to derive the parameters for $n(R)$ exploited to obtain a better estimate for the LF.

4. The radio LF

The LF for the CH87 sample obtained by using eq. (5) and the radial profile $n(R)$ determined in the previous section is illustrated in Fig. 1. It is well-represented by a 2-component power-law of the form:

$$\Phi(L) = A \begin{cases} (L/L_{\text{knee}})^{-\alpha} & \text{if } L < L_{\text{knee}} \\ (L/L_{\text{knee}})^{-\beta} & \text{if } L > L_{\text{knee}} \end{cases} . \quad (8)$$

where: $\log A = 2.12$, $\alpha = 0.92$, $\beta = 1.45$, $\log L_{\text{knee}} = 23.77$. To facilitate comparisons with published LFs, we convert our monochromatic LF (in units of $\text{erg}^*\text{sec}^{-1}\text{Hz}^{-1}$) into Lyman continuum fluxes, Q , (in sec^{-1} unit) and into $H\alpha$ luminosities, $L(H\alpha)$, (in $\text{erg}^*\text{sec}^{-1}$ unit). To convert into Lyman continuum fluxes, we make use of eq. (2) in Condon (1992) in which we assume $T_e = 6000$ K, as obtained by averaging out over the values reported by CH87. Likewise, to express the LF in terms of $L(H\alpha)$ fluxes, we use eq. (5.23) in Osterbrok (1974), together with the recombination coefficients $\alpha_{H\beta}^{eff}$, α_β and the Balmer decrements compiled by Osterbrok (1974) and Storey & Hummer (1995).

5. Discussion

The $H\alpha$ luminosities in the CH87 sample span nearly three orders of magnitudes, from $10^{36.5}$ to 10^{39} erg/sec or, in equivalent Lyman continuum luminosities, from 10^{48} to $10^{50.5}$ sec^{-1} . The lower limit corresponds to HII regions ionized by a single star, while the upper value is indicative of the lack, in our Galaxy, of *giant* and *supergiant* HII regions such as 30 Doradus in the Large Magellanic Clouds, which originate from very large OB associations. The derived LF presents a change of slope at $L_{\text{knee}} \sim 10^{23.5}$ $\text{erg}/\text{sec}^*\text{Hz}$, corresponding to an $H\alpha$ luminosity of $\sim 10^{38.3}$ erg/sec and a Lyman continuum luminosity of $\sim 10^{49.8}$ sec^{-1} (Fig. 3a and b). Above the break luminosity, the LF becomes steeper. On the contrary, for $L < L_{\text{knee}}$, the curve flattens significantly. This break has been observed by many authors. Among these, KEH were the first to conduct a systematic study of the behavior of the HII region LF by analysing 30 spiral and irregular galaxies. For 6 galaxies (of Hubble type Sab-Sb) of their sample, they find that the LF has an abrupt turnover at $\log L(H\alpha) = 38.7$ -

39.0. Recently, Bradley et al. (2006) have reported a mean value for the break luminosity of $\log L(H\alpha) = 38.6 \pm 0.1$, based on a sample of 56 spiral galaxies. Such a break has been interpreted in several fashions. KEH suggest that the change in the slope corresponds to a transition between normal HII regions (ionized by a single star or by a small association) and the class of supergiant. Oey & Clarke (1997) seem to favor the hypothesis that the break might be caused by evolutionary effects and a maximum number of stars per cluster, while Beckman et al. (2000) argue that it is due to the fact that, at luminosities above a given threshold, density bounding prevails on ionisation bounding. As for the slope of the LF, our findings are in agreement with published estimates from extragalactic studies as well as with results obtained for our own Galaxy. For instance, KEH report, for Sbc-Sc galaxies, a power-law index in the range 0.5 - 1.5 and Smith & Kennicutt (1989) find an index 1.9.

6. The IR LF

The analysis here presented will be extended by computing the IR LF by using the MIPS GAL Spitzer Legacy Survey data, i.e. a survey of the inner Galaxy (first and fourth quadrants, $|b| < 1$ deg) at 24 and $70\mu\text{m}$, carried out with the MIPS instrument on board the Spitzer Space Telescope. The comparison between the radio LF and its IR counterpart will allow to shed light on the physical relation between the free-free and the thermal dust emission inside compact HII regions.

7. Conclusions

We have investigated the LF of compact Galactic HII regions with a sample of ~ 200 sources. The sources are from the CH87 recombination line survey of the fourth quadrant and the set is complete down to ~ 3 Jy. The LF so obtained is well-represented by a two-component power law with a break luminosity at $\log L(H\alpha) = 38.3$. Remarkably, we do not see any evidence of a flattening of the LF at luminosities below $\sim \log L(H\alpha) = 37$.

This work is based based in part on observations made with the *Spitzer Space Telescope*, which is operated by the Jet Propulsion Laboratory, California Institute of Technology under NASA contract 1407.

REFERENCES

- Banfi, M., Rampazzo, R., Chincarini, G. & Henry, R. B. C., 1993, *A&A*, 280, 373
- Beckman, J. E., Rosaz, M., Zurita, A. et al., 2000, *ApJ*, 119, 2728
- Bradley, T. R., Knapen, J. H., Beckman, J. E. & Folkes, S. L., 2006, *A&A*, 459, 13
- Caswell, J. L. & Haynes, R. F., 1987, *A&A*, 171, 261
- Condon, J. J., 1992, *ARA&A*, 30, 575
- Downes, D., Wilson, T. L., Bieging, J., Wink, J., 1980, *A&AS*, 40, 379
- Eisenhauer, F., Genzel, R., Alexander, T., et al., 2005, *ApJ*, 628, 246
- Fich, M., Blitz, L., Stark, A. A., 1989, *ApJ*, 342, 272
- Haynes, R. F., Caswell, J. L., Simons, L. W. J., 1978, *Aust. J. Phys. Astrophys. Suppl.*, 45, 1
- Haynes, R. F., Caswell, J. L., Simons, L. W. J., 1979a, *Aust. J. Phys. Astrophys. Suppl.*, 48, 1
- Kennicutt, R. C., Edgar, B. K. & Hodge, P. W., 1989, *ApJ*, 337, 761
- Knapen, J. H., *MNRAS*, 1998, 297, 255
- Lockman, F. J., 1989, *ApJS*, 71, 469
- Osterbrock, D. E., 1974, *Astrophysics of Gaseous Nebulae*, ed. Freeman
- Paladini, R., Burigana, C., Davies, R. D. et al., 2003, *A&A*, 397, 213
- Paladini, R., Davies, R. D., De Zotti, G., 2004, *MNRAS*, 347, 237
- Rand, R. J., 1992, *AJ*, 103, 815
- Rozas, M., Zurita, A., Beckman, J. E., 2000, *A&A*, 354, 823
- Sanders, D. B., Solomon, P. M., Scoville, N. Z., 1984, *ApJ*, 276, 182
- Schmidt, M., 1968, *ApJ*, 151, 393
- Smith, T. R. & Kennicutt, R., 1989, *PASP*, 101, 649
- Storey, P. J. & Hummer, D. G., *MNRAS*, 272, 41